

# Motor Bearing Fault Detection Based on ICEEMDAN-EPO-SVM

Zhi Wang\*, Hao Wang, Yuan Wang

*Hohhot Power Supply Branch, Inner Mongolia Power (Group) Co., Ltd, Hohhot, Inner Mongolia, China*

*\*Corresponding Author*

**Abstract:** To address the issues of frequent damage to motor bearings and the limitations of traditional diagnostic methods, such as time consumption and low accuracy, a novel bearing fault detection strategy is proposed. This strategy integrates the Eagle Perching Optimization (EPO) algorithm for optimizing key parameters of Support Vector Machine (SVM). Initially, the Improved Complete Ensemble Empirical Mode Decomposition with Adaptive Noise (ICEEMDAN) technique is utilized to analyze vibration signals, thereby obtaining a set of Intrinsic Mode Functions (IMFs). Subsequently, correlation analysis is conducted for feature selection, followed by reconstruction, where the energy moment serves as the fault feature vector. Given that SVM classification performance is significantly influenced by the configuration of its key parameters, the EPO algorithm is utilized to optimize and determine these parameters effectively. The fault feature vectors are then classified using the EPO-optimized SVM model. Experimental results demonstrate that the proposed ICEEMD-EPO-SVM approach achieves a comprehensive fault detection accuracy of 97.5%.

**Keywords:** Motor; Bearing; ICEEMDAN; Eagle Perching Optimization; SVM

## 1. Introduction

As China's industrialization process continues to move forward, the application scope of motors across various fields is expanding, and the total number of motors in use is steadily increasing. Statistical data indicate that motors account for over 60% of the overall electricity consumption in the power grid. In industrial production, motor failures can lead to catastrophic consequences, including personal injury and significant economic losses.

Bearings, as a critical core component responsible for load-bearing and transmission in motors, are prone to failure due to complex and variable operating conditions. According to statistics, 44% of motor failures are attributed to bearing issues. Therefore, detecting motor bearing faults holds substantial engineering significance [1].

When a rolling bearing malfunctions, its signal becomes extremely complex due to the superposition of various vibration signals, including noise, high-frequency carrier waves, low-frequency modulated waves, and stress waves [2]. Furthermore, these signals primarily display nonlinear and non-stationary properties. In order to extract fault characteristics from these non-stationary signals, it is crucial to choose suitable signal processing approaches. At present, commonly employed methods encompass short-time Fourier transform, wavelet analysis, Wigner-Ville distribution, and more [3]. However, these methods lack adaptive decomposition capabilities when analyzing fault signals and require manual parameter tuning. Inappropriate parameter configurations might result in the loss or distortion of fault feature information, which can compromise the precision of fault diagnosis. To overcome this limitation, researchers have developed empirical mode decomposition (EMD), an adaptive time-frequency analysis technique. Despite its effectiveness in handling non-stationary signals, EMD is prone to challenges such as mode mixing, boundary effects, and insufficient decomposition. To alleviate these issues, Liu et al. proposed ensemble empirical mode decomposition (EEMD). While EEMD has achieved good results, it suffers from low computational efficiency and generates pseudo-components [4]. Later, Torres et al. extended the research by introducing complete ensemble empirical mode decomposition with adaptive noise (CEEMDAN), building upon

the foundations of EEMD. Although CEEMDAN improves decomposition efficiency and addresses the inefficiency of EEMD, it still faces challenges related to residual noise and pseudo-modal components. To overcome the limitations of mode aliasing and residual noise in methods like EMD, EEMD, and CEEMDAN. Colominas et al. introduced ICEEMDAN, whose primary advantage is its capability to decompose signals into more precise intrinsic mode functions (IMFs). Therefore, this study applies ICEEMDAN to fault detection. Through ICEEMDAN decomposition, the energy moments of each IMF component can be obtained and used as feature vectors. This method not only considers the temporal factor but also accounts for the energy range and distribution across different time intervals. Compared with traditional approaches that use energy entropy as fault features, this method provides a more comprehensive reflection of signal characteristics.

There are various methods for classifying motor bearing faults. Among these, the SVM algorithm has been extensively utilized in fault classification due to its robust learning capability and superior classification performance. However, SVM is highly sensitive to parameter settings, necessitating the use of intelligent optimization algorithms to optimize its critical parameters. In this study, the Eagle Perching Optimization (EPO) algorithm is employed to determine the optimal values of the penalty parameter  $C$  and kernel parameter  $\gamma$  in SVM. By integrating ICEEMDAN with energy moments of each order, accurate identification and classification of bearing faults can be achieved.

## 2. Basic Theory

### 2.1 ICEEMDAN

The ICEEMDAN algorithm is an extension of the CEEMDAN algorithm's principle [5]. It differs from the CEEMDAN method, which involves directly incorporating Gaussian white noise during decomposition, this algorithm introduces Gaussian white noise processed by EMD, effectively solving problems such as mode aliasing and noise residue, thereby significantly improving the effect of signal decomposition. Let  $s$  be the original signal

and  $E_f(\cdot)$  be the  $f$  th IMF obtained after EMD decomposition. The main steps are:

1. In the original signal sequence, a set of Gaussian white noise  $v^{(i)}$  is added to obtain the signal  $s^{(i)}$  containing controllable noise, which is expressed as:

$$s^{(i)} = s + \beta_0 E_1(v^{(i)}) \quad (1)$$

Where,  $s^{(i)} = s + \beta_0 E_1(v^{(i)})$ .

2. When  $K = 1$ , the EMD is used to calculate the first residual component  $r_1$  and the first intrinsic mode function  $IMF_1$  respectively. Their expressions are as follows:

$$r_1 = \langle M(s^{(i)}) \rangle \quad (2)$$

$$IMF_1 = s - r_1 \quad (3)$$

Where,  $M(\cdot)$  is the operator for calculating the local mean.

3. When  $k \geq 2$ , the residual component of order  $k$  is:

$$r_k = \langle M[r_{k-1} + \beta_{k-1} E_k(v^{(i)})] \rangle \quad (4)$$

Where,  $T$  represents the total number of IMF, and  $\beta_{k-1}$  is the amplitude coefficient of the  $k-1$ th noise addition.

4. Calculate the  $k$  th order modal component  $IMF_k$ , that is:

$$IMF_k = r_{k-1} - r_k \quad (5)$$

Repeat steps 3 and 4 until the decomposition is completed, thereby obtaining all the modal components and residual components.

### 2.2 IMF Energy Moment Invariant Characteristics Extraction

Research shows that the energy distribution of IMF under different bearing conditions varies. By using energy moment as the fault feature vector, it can not only reflect the magnitude of energy but also reveal its distribution characteristics on the time scale. The energy moment of each order of IMF is:

$$E_i = \sum (T \cdot k) |c_i(T \cdot k)|^2 \quad (6)$$

Where,  $T$  is the sampling period and  $k$  is the number of sampling points. The eigenvector is:

$$\{\overline{E}_1, \overline{E}_2, \dots, \overline{E}_n\} = \left\{ \frac{E_1}{\overline{E}}, \frac{E_2}{\overline{E}}, \dots, \frac{E_n}{\overline{E}} \right\} \quad (7)$$

$$\overline{E} = \sum_{i=1}^n E_i \quad (8)$$

### 2.3 Eagle Perching Optimization Algorithm

The Eagle Perching Optimization (EPO) algorithm was proposed by Ameer in 2018, and its design inspiration comes from the survival behavior of eagles in the natural environment [6]. This algorithm explores the entire area through random sampling and calculates the optimal value of the sample points by means of the objective function. Then, it further samples the optimal value to achieve the transition from global search to local fine search. The EPO algorithm has a clear principle, is easy to implement, and belongs to a new type of swarm intelligence optimization method. Moreover, it has the advantage of fast convergence.

The eagle is a general term for various large carnivorous birds belonging to the Accipitridae family and is a typical carnivorous animal. Male eagles prefer to perch at high places, such as tall trees, steep cliffs or lofty mountains. They are innately endowed with an ability similar to an algorithm, enabling them to precisely locate the highest points. The hunting strategy of eagles is quite unique: they soar to high altitudes for observation and select samples at multiple locations, determine the highest point and then fly towards it, and further collect information to calibrate the optimal position. By repeating this process and constantly making fine adjustments, eagles can eventually find the best habitat. In the EPO algorithm, the initial position of each eagle is randomly generated, which ensures the uniform distribution of the population throughout the search space, thereby providing favorable conditions for the optimization process. The initial position can be expressed as:

$$x = l_b + (u_b - l_b) \times r \quad (9)$$

Where,  $x$  represents the initial position, and  $u_b$  and  $l_b$  are the upper and lower bounds for optimization, respectively.

The search range variable of the EPO algorithm is updated to:

$$s = s \times e \quad (10)$$

Where,  $s$  is the search range variable and  $e$  is the search variable, specifically:

$$e = (I_{res} / s) \frac{t}{t_s} \quad (11)$$

Where,  $I_{res}$  is the resolution range.

The updated position of each eagle is:

$$x_i^{t+1} = x_{min}^t + \Delta x_i \quad (12)$$

$$\Delta x_i = s \times (R_{i,1}, R_{i,2}, \dots, R_{i,n}) \quad (13)$$

Where,  $R_{in}$  is a random number and  $x_{min}^t$  is the global optimal position when the iteration reaches the  $t$ th time.

### 2.4 SVM

The key of SVM lies in finding a separating hyperplane, which can not only accurately classify the training data set but also ensure that the obtained geometric margin reaches the maximum value [7]. The main function expression form is:

$$\begin{cases} \min \|\omega\|^2 / 2 + C \sum_{i=1}^n \varepsilon_i \\ s.t. y_i (\omega x_i + b) \geq 1 - \varepsilon_i \\ \varepsilon_i \geq 0 \quad i = 1, 2, \dots, n \end{cases} \quad (14)$$

Where,  $\omega$  represents the weight,  $x_i$  the training sample,  $y_i$  the sample type,  $b$  the threshold,  $C$  the penalty function, and  $\varepsilon_i$  the slack factor. By utilizing Equations (8) and (14), and through the introduction of the Lagrange function, the duality principle, and the kernel function, the decision function for the SVM can be established. Its specific expression form is:

$$f(x) = \text{sgn} \left\{ \sum_{i=1}^n y_i a_i K(x_i, x) + b \right\} \quad (15)$$

$$K(x_i, x) = \exp \left[ -\theta \|x_i - x\|^2 \right] \quad (16)$$

## 3. Experimental Analysis

### 3.1 Experimental Procedures

The procedure for the fault detection based on ICEEMDAN-EPO-SVM is described below:

1. Collect the vibration signals of the bearing under four distinct operating conditions.
2. Process the vibration signals using ICEEMDAN and select the useful IMF components for reconstruction.
3. The energy moment of the reconstructed signal is calculated as the fault feature vector and divided into the training set and the test set.
4. Use EPO to optimize the key parameters of SVM.
5. The trained EPO-SVM model is utilized to classify the test set samples, thereby achieving

fault detection.

### 3.2 Experimental Data

In order to validate the efficacy of the proposed approach, this study employed the bearing dataset supplied by the University of Western Reserve for experimental analysis. The bearing model selected for the experiment was 6205-2RS JEM SKF, with a motor speed set at 1730 r/min. The sampling frequency was set at 12 kHz, with a load condition of 0 HP. Various types of single-point damage were introduced to the rolling bearing using electrical discharge machining technology. The collected vibration data encompassed four distinct fault states, with 100 samples selected for each state, and each sample having a data length of 1024.

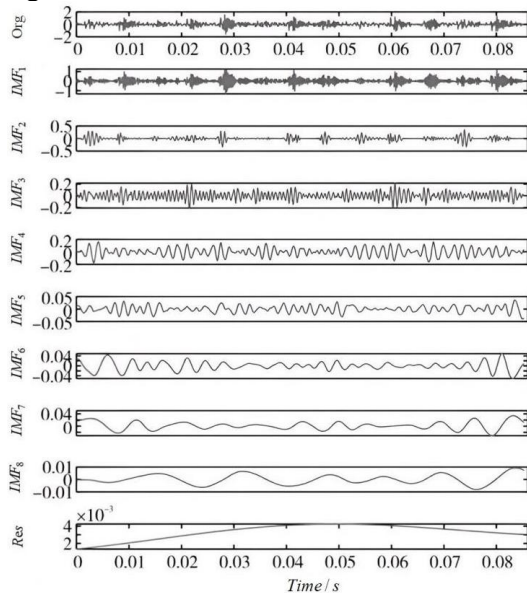


**Figure 1. Decomposition Results of CEEMDAN for Inner Ring Faults**

Using the vibration signal of an inner ring fault as a case study, the CEEMDAN method was first applied to decompose the signal. More specifically, the ratio of noise standard deviation to the original data standard deviation was established at 0.3, the number of noise additions for iteration was set to 50, and the maximum number of iterations was capped at 200. The decomposition outcomes are illustrated in Figure 1, generating a collection of intrinsic mode functions (IMFs). Under identical parameter settings, the ICEEMDAN decomposition results are shown in Figure 2. By comparing Figure 1 and Figure 2, it is evident that both methods successfully decomposed the vibration signal into 8 IMFs

and 1 residual component. This effectively reconstructed the waveform features of the original signal while resolving the mode mixing problem commonly associated with traditional EMD decomposition. However, the results indicate that IMFs 5, 6, and 7 obtained via CEEMDAN decomposition were affected by endpoint effects, leading to some degree of waveform distortion. In contrast, no such distortion was observed in the time-domain waveforms of the IMFs obtained through ICEEMDAN decomposition. This demonstrates that the ICEEMDAN method effectively mitigates the influence of endpoint effects.

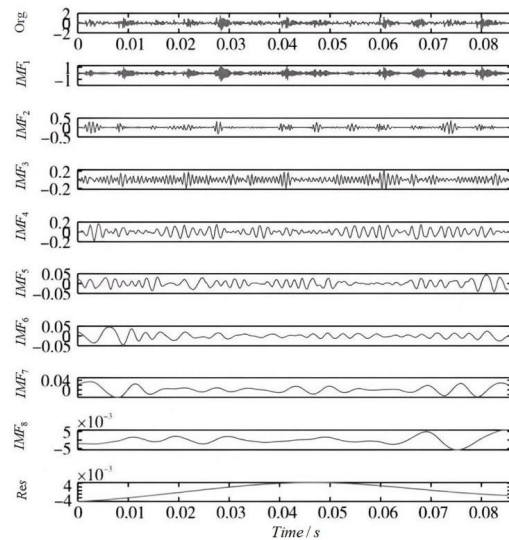


**Figure 2. ICEEMDAN Decomposition Results of Inner Ring Faults**

The correlation coefficients between each IMF component and the original vibration signal were computed, and the results are displayed in Table 1. As indicated in Table 1, the correlation coefficients of the IMF components obtained using the ICEEMDAN method are consistently higher than those derived from the CEEMDAN decomposition method. Generally, a larger correlation coefficient indicates a higher degree of similarity between the component and the original vibration signal. Upon calculation, the correlation coefficient thresholds for the two decomposition methods were determined to be 0.1629 for ICEEMDAN and 0.1378 for CEEMDAN, respectively. IMF components whose correlation coefficients surpassed the respective thresholds were chosen for signal reconstruction. Following this, the multi-scale permutation entropy feature vectors of the bearing were extracted based on the reconstructed signal.

**Table 1. The Calculation Result of the Correlation Coefficient**

| Method   | IMF1  | IMF2  | IMF3  | IMF4  | IMF5  | IMF6  | IMF7  | IMF8  |
|----------|-------|-------|-------|-------|-------|-------|-------|-------|
| CEEMDAN  | 0.872 | 0.378 | 0.427 | 0.426 | 0.276 | 0.167 | 0.027 | 0.016 |
| ICEEMDAN | 0.983 | 0.532 | 0.632 | 0.572 | 0.426 | 0.293 | 0.092 | 0.021 |

From every sample of each bearing state, 60 subsets were randomly chosen to create the training dataset, whereas the remaining 40 subsets served as the testing dataset. In the SVM model, the radial basis function was utilized as the kernel function. During the optimization of the SVM using EPO, the penalty factor  $C$  was confined to the range of [1, 100], while the kernel function parameter  $g$  was limited to [0, 30]. The EPO optimization process was configured with 100 iterations. Additionally, cross-validation was employed to identify the most suitable values for the penalty factor  $C$  and the kernel function parameter  $g$ .

The ultimate classification outcomes of the EPO-SVM model are presented in Figure 3. In this figure, label 1 corresponds to the normal condition, label 2 indicates the inner ring fault condition, label 3 denotes the outer ring fault condition, and label 4 signifies the rolling element fault condition.

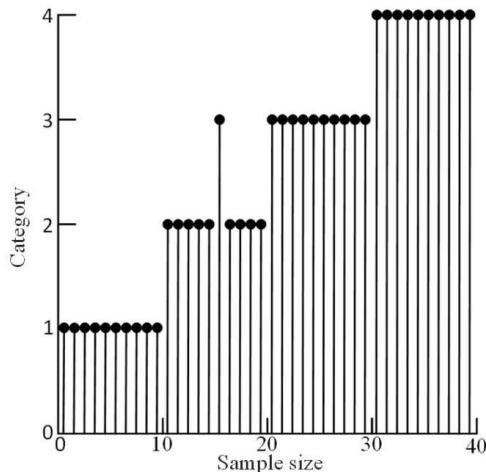
**Figure 3. Classification Results of ICEEMDAN-EPO-SVM**

Figure 3 illustrates that among the four operational states, the detection accuracy for the normal state is 100%, the accuracy for identifying inner ring faults is 90%, and the accuracy for both outer ring faults and rolling element faults is 100%. Additionally, the detection accuracy for comprehensive faults is 97.5%.

#### 4. Conclusion

In order to tackle the problems of prolonged

detection time and insufficient detection accuracy in bearing fault diagnosis, a new fault detection approach based on ICEEMDAN-EPO-SVM is introduced. First, the ICEEMDAN technique is utilized to break down the bearing vibration signal into several IMF components. Subsequently, feature selection is performed using the correlation coefficient method, followed by signal reconstruction. The energy moment is subsequently chosen as the feature vector and fed into the SVM model for fault classification. However, given that the key parameters of the SVM method significantly influence its fault classification performance, EPO is introduced to determine the parameters of the SVM. Finally, the EPO-SVM model is utilized for fault classification and detection. The total fault detection rate achieves 97.5%, which indicates the efficiency of the proposed approach in performing precise bearing fault diagnosis.

#### References

- [1] Wang X, Li J, Jing Z, et al. Fault diagnosis method of rolling bearing based on SSA-VMD and RCMDE. *Scientific Reports*, 2024, 14(1):30637-30637.
- [2] Song J, Nie X, Wu C, et al. A Novel Intelligent Fault Diagnosis Method of Rolling Bearings Based on the ConvNeXt Network with Improved DenseBlock. *Sensors*, 2024, 24(24):7909-7909.
- [3] Feng Y, Liu P, Du Y, et al. Cross working condition bearing fault diagnosis based on the combination of multimodal network and entropy conditional domain adversarial network. *Journal of Vibration and Control*, 2024, 30, (23-24):5375-5386.
- [4] Li K, Chen X, Hu X, et al. Failure Libration Model of Bearing And Its Fault Diagnosis Based on EMD//IEEE, IEEE Beijing Section. *Proceedings of 2013 IEEE 4th International Conference on Software Engineering and Service Science. Joint Laboratory of Ocean-based Flight Vehicle Measurement And Control China Satellite Maritime Tracking and Control Department*, 2013, 1028-1031.
- [5] Lin J. Improved Ensemble Empirical

- Mode Decomposition and its Applications to Gearbox Fault Signal Processing. International Journal of Computer Science Issues, 2012, 9(6):194-199. DOI:10.1007/978-3-642-27869-3\_14.
- [6] Ralhan S, Singh M, Sahu N, et al. Comparative Analysis of FOPI Controller using Eagle Perching Optimization for Fuel Cell connected Distributed Generation System. 2021. DOI:10.1109/ICAECT49130.2021.9392443.
- [7] Hong T, Hongliang D, Yi D. Tapered Roller Bearing Failure Diagnosis Based on Improved Probability Box Model. IEEE ACCESS, 2020, 8151452-151464.